

A contribution to the basic understanding of nucleate boiling phenomena: generic experiments and numerical simulations

Peter Stephan^{†‡}, Axel Sielaff[†], Sebastian Fischer[†], Jochen Dietl[†] and Stefan Herbert[†]

Abstract

Since Nukiyama's pioneering experiment and findings in the 1930s many researchers have further investigated the boiling process and developed empirical or semi-empirical methods to predict the boiling heat transfer coefficient. However, several details of the local heat transport phenomena are still not fully understood. The heat transfer from the heated wall to the bulk fluid is extremely complex and many aspects are involved: nucleation, dynamic wetting characteristics, surface tension and other fluid properties, gravitation, bulk subcooling, etc...

Only in the recent years experimental methods reached spatial and temporal resolutions that allow observing the boiling process on the scales of these individual aspects and local dynamic phenomena in the two-phase boundary layer. Similarly, numerical methods reached a level of robustness and resolution that allows studying the influence of these aspects and phenomena in a computer simulation. This work will give an overview on recent developments and modern experimental and numerical methods nucleate boiling heat transfer research, Results from combined generic experiments and numerical simulations are presented. They give a deep insight into the local and transient transport phenomena in the two-phase boundary layer.

Key Words: *Nucleate boiling, Vapor bubble, Departure diameter, Conjugated heat transfer*

NOMENCLATURE

c	:	thermal capacity
k	:	thermal conductivity
q	:	heat flux
T	:	temperature
x, y	:	cartesian coordinates
α	:	thermal diffusivity
ξ, η	:	local coordinates
δ	:	thickness
ρ	:	density
τ	:	time
subscripts		
0	:	input
s	:	solid

INTRODUCTION

Boiling is an important phase change and heat transfer method with a wide variety of technical applications. Probably each and every undergraduate course on boiling heat transfer worldwide starts with a presentation and

further discussion of the *Nukiyama Curve* which describes the relation between wall superheat ΔT compared to saturation temperature and the heat flux q in the different pool boiling regimes. This curve was presented in 1934 by Shiro Nukiyama in his pioneering paper entitled "The Maximum and Minimum Values of the Heat Q Transmitted from Metal to Boiling Water under Atmospheric Pressure". Nukiyama (1934) found this characteristic relation in an experiment using an electrically heated metallic wire evaluating accurately temperature and heat flux. Nukiyama's work became a guideline to heat transfer engineering for the design and control of boilers and/or steam generators. Important heat transfer states such as the onset of nucleate boiling (ONB), the critical heat flux (CHF), and the Leidenfrost temperature are related to characteristic changes in the slope of the *Nukiyama Curve*.

Received: February 7, 2013, Editor : Katsunori Hanamura

[†] Institute of Technical Thermodynamics, TU Darmstadt, Petersenstr. 17, D-64287 Darmstadt, Germany

[‡] Center of Smart Interfaces, TU Darmstadt, Petersenstr. 17, D-64287 Darmstadt, Germany

Since Nukiyama's work many researchers have studied boiling heat transfer experimentally, theoretically and later also numerically. Their focus was mainly the investigation of the nucleate boiling regime, i.e. the regime in between ONB and CHF, because this regime is the most important one in the majority of applications. As a result quite a huge number of empirical correlations for the heat transfer coefficient $h=q/\Delta T$ were published for many specific cases. These correlations are the basis of today's design methods, but typically they are only reasonably accurate for certain fluids in a limited range of process parameters, because they do not entirely describe the complex and dynamic two-phase transport phenomena and their interaction. The reason for that is very simple and astonishing at the same time after almost hundred years of boiling research: the complex and dynamic two-phase transport phenomena and their interaction are still not fully understood. However, it is generally accepted in the scientific community that the following transport phenomena play a role during vapor bubble growth and detachment:

- Transient conduction from the superheated liquid boundary layer to the liquid-vapor interface
- Evaporation at the liquid-vapor interface in the superheated near wall region
- 'Micro layer' evaporation in the thin film region near the moving contact line at the foot of the bubble
- Partial recondensation of vapor when the bubble moves out of the superheated boundary layer in case of a subcooled bulk region
- Forced convection induced by the moving interface (flow of colder liquid from the bulk into the wake of the rising bubble)
- Natural convection and buoyancy
- Marangoni convection due to temperature gradients
- Transient heat conduction in the solid wall underneath the bubble
- Diffusive mass transfer and Marangoni convection due to concentration gradients in case of fluid mixtures

However, which of these transport phenomena dominate under which process conditions is partially still an open question. Moreover, the heterogeneous bubble nucleation process is even less understood and an a priori prediction of the active nucleation site density is still impossible. In a rather recent review paper, published in a special issue on boiling heat transfer, Manglik (2006) listed the numerous influencing parameters on nucleate

boiling heat transfer. He attributed these parameters either to the fluid (fluid properties, liquid-vapor phase change characteristics, etc.), to the solid heater (thermophysical properties, roughness, etc.) or to the heater-fluid interface (wettability, active site density, etc.). With that it becomes very obvious that the heat transport process is extremely complex. Thus, purely empirical research and global measurements, i.e. time and space averaged temperature and heat flux observations, similar to Nukiyama's pioneering work are still justified to characterize nucleate boiling heat transfer for new wall surfaces (e.g. microstructured surfaces) or new fluids (e.g. nanofluids). However, the tremendous progress in measurement techniques as well as in numerical methods and computer performance since about a decade or so today allows a detailed investigation of the nucleate boiling process with high spatial and temporal resolution. This opens a path towards a deeper basic understanding of the local transport phenomena and may lead to more physically based prediction methods in future.

In the following sections the authors present a series of very generic nucleate boiling experiments using high resolution measurement techniques and closely aligned numerical simulations that include multiple characteristic scales of the boiling process.

2. STATE OF THE ART REVIEW

2.1 Generic experiments

In the past two decades measurement techniques with high temporal and spatial resolution have become available. Ensuing this development, many researches involved in experimental investigations of nucleate boiling redirected their focus from global measurements of heat transfer to the more fundamental aspect of investigating heat transfer at single bubbles. Today, it is broad consensus in the scientific community that in order to understand the physical process of nucleate boiling, one first has to gain deeper understanding of the phenomena involved in single bubble heat transfer. Apart from gaining insight into phenomena, single bubble experiments additionally can be used to develop and validate numerical models for single bubble heat transfer. Such numerical models allow determining phenomena on geometric and temporal scales that are still not accessible through ex-

periments, but might have a major impact onto the process.

The group around Dhir conducted experiments on the influence of wall superheat and liquid subcooling on bubble growth rates and liftoff behavior. Qiu et al. (2002) carried out experiments on the growth and departure dynamics of single water vapor bubbles growing on an artificial nucleation site on a heated and polished silicon wafer. They found that the wall superheat has – if any – only a small effect on the equivalent bubble departure diameter, while increasing liquid subcooling seems to result in a slight decrease of the bubble departure diameter. However, it was found that the bubble growth time decreases significantly with increasing wall superheat and increases with increasing liquid subcooling. Of course, bubble departure radius and frequency depends on gravitational buoyancy forces. Recently Dhir et al. (2012) carried out nucleate boiling experiments on the International Space Station (ISS) under very good microgravity conditions with gravity levels between $6 \times 10^{-7} g_E$ and $1.2 \times 10^{-7} g_E$ (g_E being the earth gravitational acceleration). It was observed that for low wall superheats lateral bubble mergers led to one big single bubble attached to the heater surface acting as a heat sink through vapor recondensation at the bubble cap. At higher wall superheats however, the big bubble detached from the wall and merged with smaller bubbles generated on the heater surface sucking them away from the wall. This shows the importance of bubble coalescence on the overall heat transfer, at least in the absence of buoyancy.

Siedel et al. (2008) used a 40 μm thin circular copper plate with a diameter of 18 mm which is soldered to a copper cylinder heated by a cartridge heater. The boiling surface was polished and an artificial cavity placed in the center. The single bubble growth dynamics were observed using a high speed camera. For high wall superheats an oscillation of the bubble was detected. It was found that the bubble growth time depends on wall superheat, whereas the detachment volume is independent, which is in accordance with the findings of Qiu et al. (2002).

Hutter et al. (2010) used a silicon wafer with integrated micro-sensors and single etched artificial cavities (40 to 100 μm in depth, 10 μm in width). The bubble di-

ameter and frequency as well as the heat flux and waiting time between bubble detachment and subsequent bubble nucleation were evaluated for different cavity depths. Using a similar setup measurements with multiple artificial cavities and interacting neighboring bubbles were performed (Hutter et al., 2012).

Kim et al. (2002) carried out experimental investigations of pool boiling phenomena using silicon microheater arrays consisting of small rectangular platinum resistance heaters. Two different quadratic microheater arrays were employed: one with 7 mm side length and one with 2.7 mm side length. Each microheater array consisted of 10 by 10 single microheater elements, thus, the microheater size was 0.7 mm or 0.27 mm, respectively. Through a feedback loop, each element of the array could be run either in constant heat flux or constant temperature mode, allowing measurement of the other quantity. It should be noted that while the mean heat flux or temperature across each microheater element was kept constant or measured, the local distributions across each microheater remained unknown. Using these heater arrays in microgravity experiments during parabolic flights Raj and Kim (2010a) found a characteristic threshold value: the ratio of the lateral heater size to the fluid capillary length L_H / L_C . Pool boiling heat transfer below $L_H / L_C \approx 2.1$ was found to be heater size dependent, whereas above this threshold value no influence of the lateral heater size could be determined by Raj and Kim (2010a) and Raj et al. (2010b). Delgoshaei and Kim (2010) analyzed the transient heat flux from single microheater elements of the array and calculated an equivalent bubble departure diameter: The calculation was based on the assumption that all heat from the heater elements below the bubble is transferred through contact line and/or microlayer evaporation into latent heat of the vapor. This equivalent bubble diameter was compared to the physical bubble diameter taken from bubble images. A physical diameter larger than the equivalent one was attributed to additional evaporative heat transfer from the superheated liquid. They found that long bubble growth times and short waiting times between two successive bubble growth periods promoted the contribution from wall heat transfer, while ebullition cycles with short waiting times are dominated by evaporation from the superheated liquid layer.

Auracher and Buchholz (2005) developed a heater with implemented constantan/copper microthermocouples. For local measurements of the surface temperature a 6 by 6 grid of thermocouples with an individual diameter of 38 μm and a spacing of 0.2 mm in between was used. The thermocouple connection was only 3.6 μm underneath a gold coated boiling surface. To calculate the local heat flux from the transient local temperature measurements a 3D inverse heat transfer method was developed and used in cooperation with Marquardt's group (Heng et al., 2008, 2010, 2011). The measurements indicated that a substantial amount of heat is removed from the heater in the contact line region. Additional measurements using microoptical probes and gold/constantan microthermocouples with a diameter of only 12.7 μm in the 2-phase fluid were conducted by Auracher and Buchholz (2005). The microoptical probes were fabricated of an etched glass fiber. Due to the different refraction indexes of liquid and vapor, a phase detection at the tip could be performed. Because of their small dimensions the influence of the probes onto the boiling process was assumed to be small. The small thermal mass of the tiny microthermocouple enabled measurements at a much higher measurement frequencies than applying commercial thermocouples. Void fraction and the temperature fluctuations near the surface were measured.

Tadrist et al. analyzed heat transfer to single bubbles with special emphasis to the contribution of Marangoni or thermocapillary convection. By injecting air bubbles from an orifice onto a downward facing heater wall at different Marangoni numbers Arlabosse et al. (2000) found that the ratio of heat transferred from the wall with a bubble to heat transferred without a bubble increased with rising Marangoni number. In this study the heat flux was measured using a heat flux meter, thus time and space averaged values were recorded. The flow profile around the bubbles was characterized applying particle image velocimetry (PIV). It was found that the maximum Reynolds number of the induced flow scales linearly with increasing Marangoni number for constant Bond and Prandtl numbers. Reynard et al. (2001, 2005) studied 3D oscillatory thermocapillary convection patterns around an air bubble injected close to a heated wall. Within the experiments a threshold value for the onset of

3D oscillatory thermocapillary convection was characterized based on a critical bubble radius and a critical temperature gradient. Barthès et al (2006) studied heat transfer to single vapor bubbles and Marangoni convection patterns in degassed and non-degassed fluid using shadowgraphy and a heat flux meter to measure the time-resolved average heat flux from a downward facing heater wall to the fluid. In the non-degassed case convection instabilities were observed. They were attributed to thermocapillary convection.

The group of Di Marco conducted experiments under normal gravity (earth) and microgravity with the main focus on the evaluation of the forces acting on a growing vapor bubble and the effect of an electrical field on the force balance. It was shown that an electrical field can result in an additional force for bubble detachment, and thus has a potential to replace the gravitational force during boiling heat transfer in space applications. Di Marco and Grassi (2002) reported an increase of critical heat flux CHF with electrical field intensity (represented by the applied voltage) under microgravity. With high voltages applied ($U_{\text{elec. Field}} \approx 10 \text{ kV}$), CHF under microgravity was comparable to CHF under normal gravity without electrical field. These measurements were carried out using horizontal platinum wires of different diameters ranging from 0.2 to 0.6 mm, which served as both, resistance heater and resistance thermometer, so only global results and no results for single bubbles could be obtained. Di Marco et al. (2003) carried out experiments with single nitrogen bubbles injected into FC-72 and subjected to electrical fields of varying intensity under normal gravity and microgravity conditions. Di Marco et al. (2012a) presented a force balance including the electrical field force, buoyancy, internal bubble pressure and surface tension forces. It was found that the presence of an electric field does not only exert a force onto the bubble, but also influences the bubble shape, changing the other terms of the force balance. For an upward facing surface configuration Di Marco (2012b) reported an elongation of the generated nitrogen bubbles through the electric field, leading to an increase of the internal bubble overpressure.

Starting in the early 1990s Kenning et al. used thermo-chromic liquid crystal (TLC) thermography to investigate pool boiling processes. As the color of the liquid

crystals changes with temperature local temperature measurements could be performed. Due to the extremely small size of the crystals the spatial resolution mainly depends on the resolution of the camera. Kenning and Yan (1996) used a 0.13 mm thick stainless steel plate as boiling surface which was heated electrically. The plate was coated with unencapsulated liquid crystals on the backside. The colors of the TLC layer and the bubble dynamics were recorded with 200fps using a high speed camera. The local temperature field was derived from the local color field and used to calculate the local surface heat flux by means of the following two dimensional energy balance for the wall material:

$$q = q_0 + k_s \delta_s \left(\frac{\partial^2 T}{\partial x^2} + \frac{\partial^2 T}{\partial y^2} \right) - \rho_s c_s \frac{\partial T}{\partial \tau}. \quad (1)$$

Herein, q is the surface heat flux, q_0 the input heat flux, δ_s the wall thickness, and k_s , ρ_s and c_s the thermal conductivity, density and specific heat of the solid heater material, respectively. Kenning pointed out that the local heat removal by growing bubbles induces a transient temperature variation of the heating surface. Using the same measurement technique Kenning et al. (2001, 2009) also performed experiments with sliding bubbles along a tilted plate. He reported differences in wall temperature profiles below the bubbles on horizontal and vertical heaters.

Theofanous et al. (2002) used Infrared (IR) thermography to measure the wall temperature field during boiling on top of a transparent 130 μm borosilicate glass coated with a titanium layer of 140 to 1000 nm thickness.

Golobic et al. (2009, 2012) used an electrically heated thin metal foils together with IR thermography to measure the 2D temperature field underneath the foil. The small heat capacity of the heater and the absence of the liquid crystal layer compared to Kenning's earlier studies led to a smaller temperature difference between the temperature measurement plane and heater/fluid interface. For evaluation of the local heat flux a 2D energy balance (see equation (1)) was used. Golobic also mentioned a potential disadvantage of the thin foil heater: boiling heat transfer on such thin foil heaters might be deteriorated compared to massive heaters with higher

thermal capacity. In a similar setup Golobic and Gjerkes (2001) heated the foil not electrically but with laser radiation from underneath. Heating different locations of the foil allowed activating multiple bubble nucleation sites and investigating interactions between them.

Geradi et al. (2009, 2010) used IR thermography to observe the temperature distribution on the surface of an Indium Tin Oxid (ITO) coated sapphire glass. This allowed for the simultaneous observation of the bubble from underneath with a high speed black and white camera. Using this IR-transparent heater Kim and Buongiorno (2011a, 2011b) measured the thickness of the liquid layer underneath a growing bubble applying an interferometry technique. The interference fringe pattern is caused by passage of the light through the thin film and can be observed through the transparent heater. The film thickness was calculated by evaluating the interference wavelength. Using the same technique a DEtection of Phase by Infrared Thermometry (DEPIcT) was done. Duan et al. (2012) performed PIV measurement during nucleate boiling to visualize the velocity distribution around bubbles. It was found that the velocity on top of the bubble is generally higher than at its bottom.

Sodtke et al. (2006a, 2006b) measured the local wall temperature below growing vapor bubbles under normal gravity and under microgravity conditions. They employed a 10 μm thin stainless steel foil as resistance heater. On the backside of the foil a thin TLC layer was applied to record the color field with a high speed camera. Using an in-situ calibration method the RGB color values could be mapped accurately to the 2D temperature field. Figure 1 shows a typical temperature distribution near the bubble foot along the contact line area under normal gravity and microgravity conditions. A comparison of the measured temperature drop near the bubble foot to the temperature drop predicted numerically from a model by Stephan and Hammer (1994) yielded good qualitative agreement. The measurement technique was later adapted and expanded by Wagner et al. (2007, 2008) and Schweizer and Stephan (2009). They replaced the TLC temperature measurement technique by IR thermography and included a method for local heat flux calculation. This heat flux calculation is based on a 2D energy balance for each pixel of the temperature field, approximating the partial derivatives through a finite

differences scheme. This technique relies on the assumption that the temperature difference across the foil can be neglected due to the very small thickness of the foil (Schweizer, 2009). Wagner et al. (2007) used a micro-thermocouple (MTC) to measure the transient temperature in a single vapor bubble as well as the temperature in the liquid in the wake of the bubble. A characteristic result is shown in Fig. 2. They found that, as soon as the MTC penetrates the bubble, the measured temperature drops from the superheated liquid temperature to saturation temperature or little above inside the vapor bubble. In the liquid phase in the wake of the bubble the temperature slowly rises towards the initial superheat before the bubble was penetrated.

Schweizer and Stephan (2009) reported a heat flux peak at the bubble foot related to enhanced contact line heat transfer using FC-72 as a working fluid. It was reported that during a bubble coalescence a liquid drop remained in the center of the coalesced bubble. Mukherjee and Dhir (2004) who used water as working fluid did not report such droplet generation during bubble mergers. A possible explanation for this discrepancy might be the very different surface tensions of the working fluids.

Wagner and Stephan (2008) used the same heat flux determination technique to study the effect of binary mixtures onto single bubble heat transfer. Their hypothesis was that the well-known heat transfer degradation of binary mixtures compared the pure components is related to local concentration gradient near the moving contact line. Indeed their study indicates that the local rise in

saturation temperature at the contact line due to the accumulation of the less volatile component tends to decrease the local superheat.

2.2 Numerical simulations

Due to the small length and time scales involved in boiling processes the possibilities to gain insight by measurements are still limited. Numerical simulations theoretically do not have limitations in resolving time and space, and therefore are a promising method to study the local transport phenomena in boiling systems. However, to perform accurate simulations appropriate models for the complex physics involved have to be developed.

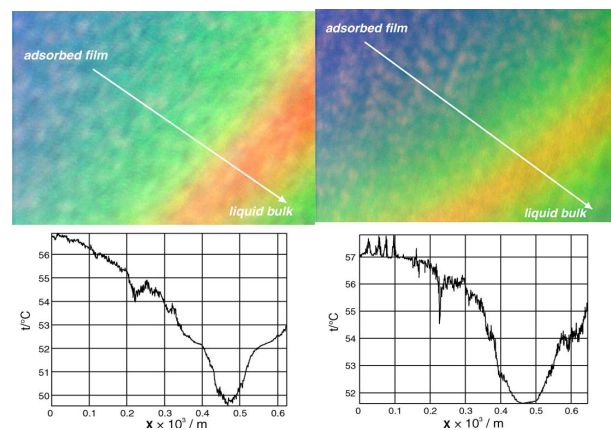


Fig. 1 Color play of TLCs and local temperature drop below the 3-phase contact line of a growing bubble under low gravity (left) and normal gravity (right) (Sodtke et al. 2006b)

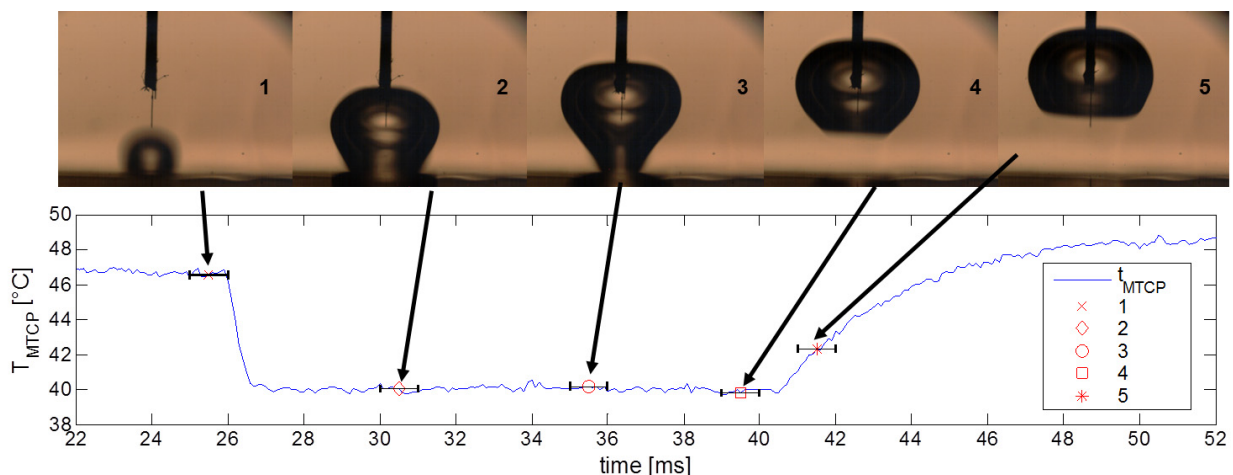


Fig. 2: Temperature measurement with microthermocouple (MTC) in the near wall 2-phase boundary layer (1: above growing bubble, 2-4: inside the bubble, 5: in the wake of the rising bubble); Fluid: HFE-7100 at 500 mbar ($T_{sat}=40^{\circ}\text{C}\pm 0.5\text{K}$)

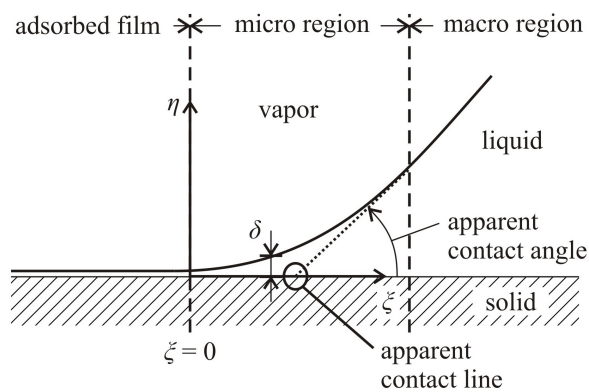


Fig. 3 Definition of the micro region from Kunkelmann and Stephan (2010a)

Besides the modeling of heat transfer within the solid and fluid phase and the representation of phase change an appropriate handling of contact line heat transfer is an important part of boiling heat transfer modeling. As the film thickness of the liquid meniscus underneath a bubble attached to the wall tends to zero at the contact line, the heat transfer resistance gets very small in the contact line area. This results in a very high heat flux in this so-called micro region. Despite of the small dimensions of the micro region a considerable part of the overall heat transfer can occur near the contact line. Kunkelmann and Stephan (2010a) found about 20% of the total heat to be transferred in the micro region. Fuchs et al. (2006) even reported a value of 32%.

The present models for contact line heat transfer by Stephan and Busse (1992) and Lay and Dhir (1995) are based on the concept of Potash and Wayner (1972). As illustrated in Fig. 3, on a microscopic scale there is no actual contact line, but the liquid meniscus turns into an adsorbed film of liquid molecules sticking to the wall because of attractive intermolecular forces. The transition region between the adsorbed film and the macro region is referred to as the micro or interline region. The typical length scale of this region is less than 1 μm . Therefore this region is not directly included into boiling simulations but a subscale model is derived which can be used in the macroscopic simulation.

The conservation equations for mass and momentum in the liquid film are simplified using the lubrication approximation. The intermolecular forces are captured by using the disjoining-pressure concept. The energy equation is solved assuming one-dimensional heat con-

duction in the liquid film but accounting for the interfacial heat resistance and the effect of disjoining pressure and curvature on the liquid-vapor equilibrium.

In the beginning of numerical research on pool boiling, quasi-stationary simulations of the heat transfer close to a bubble attached to a heated wall were investigated by Stephan and Hammer (1994). In their simulations the liquid-vapor interface was represented by a boundary of the grid. The heat conduction within the heater is also accounted for. Bubble growth and departure processes were not included directly, but the heat transfer for bubbles of different size attached to the heater could be calculated separately. Convective heat transfer and energy storage in the liquid were neglected. This approach was extended from pure fluids to binary mixtures by Kern and Stephan (2003). To extend the model to transient effects, Fuchs et al. (2006) added an arbitrary Lagrangian-Eulerian (ALE) kinematic description to account for bubble growth and detachment. The liquid vapor-interface was moved according to the actual evaporation rate assuming a spherical bubble shape. Convective heat transfer and energy storage in the liquid were included. To allow the results for heat transfer to be independent of the initial conditions chosen, several successive bubble cycles were calculated with a predefined waiting time between bubble detachment and nucleation. A significant variation of the heat stored in the wall with time was found. A different model using ALE mesh motion was developed by Welch (1998). He assumed a pinned contact line during the bubble growth and did not use a specific model for the contact line heat transfer.

Bai and Fujita (2000) as well employed the ALE method to simulate bubble growth. They assumed an isothermal wall and made use of the model for evaporation in the micro-region introduced by Stephan and Hammer (1994). The influence of subcooling and reduced gravity on flow dynamics and heat transfer were studied and a variation in bubble growth rate and shape could be observed.

Big progress in performing transient simulations was made by the development of Eulerian representations of the interface on a fixed grid, which allows more drastic changes in the interface topology than the moving mesh approach does. One of these methods is the Volume of Fluid (VoF) method developed by Hirt and Nichols

(1981) which became applicable through the handling of surface tension effects proposed by Brackbill et al. (1992). In addition, the level-set method by Osher and Sethian (1988) or front tracking methods using markers by Harlow and Welch (1965) were used. The latter one was used by Esmaceli and Tryggvason (2004), but their simulations were limited to the case of film boiling. Furthermore, a gridless method has been proposed by Yoon et al. (2001) for nucleate boiling simulation.

Important contributions using the level-set method were done by the group of Dhir. Son et al. (1999) used a level-set formulation to calculate the effect of the static contact angle and the wall superheat on bubble dynamics. They accounted for the contact line heat transfer but assumed an isothermal wall. The waiting time between two successive bubbles was prescribed. Good agreement of their numerical and experimental data was shown. This model was further used to study the effect of liquid subcooling (Dhir, 2001, Wu et al., 2007) and the presence of contaminants (Bai and Dhir, 2001). Moreover, Son et al. (2002) investigated the occurrence of vertical bubble mergers between two successive bubbles. Lateral bubble mergers were analyzed by Mukherjee and Dhir (2004). Mukherjee and Kandlikar (2007) used the same model to study the effect of a dynamic contact angle on bubble dynamics. They found mainly the advancing contact angle to have influence on the growth rate. Wu and Dhir (2010) further investigated the effect of liquid subcooling on the bubble growth. In particular, for low gravity conditions they found steady state bubbles at which conden-

sation at the bubble tip and evaporation at the bubble foot compensate. Aktinol and Dhir (2012) extended the model to account for the transient heat conduction within the heater. The waiting time was no longer prescribed, but nucleation was tied on a certain wall superheat at the position of the nucleation site. The authors found the wall thickness and material to influence the waiting time significantly.

A computational model for the simulation of nucleate boiling utilizing the VoF method was developed by Kunkelmann and Stephan (2009, 2010a, 2010b). They accounted for the coupled heat transfer between the fluid and a thin steel foil used as heater and included a model for the contact line heat transfer. The static contact angle and the waiting time were prescribed according to experiments. Similar to Fuchs et al. (2006) and Son et al. (1999) multiple successive bubble cycles were calculated to obtain results independent of the initial conditions. Good agreement of numerical and experimental results was achieved (Kunkelmann and Stephan, 2010a). A significant temperature minimum at the heater surface at the position of the contact line could be observed. Furthermore, a strong dependency of the near contact line heat transfer on the direction of motion of the bubble foot was found. In particular, the highest local heat flux was reached during the bubble detachment, i.e. in an advancing contact line situation. This behavior has been confirmed through combined experiments and simulations by Kunkelmann et al. (2012) for various configurations in which moving contact lines appear.

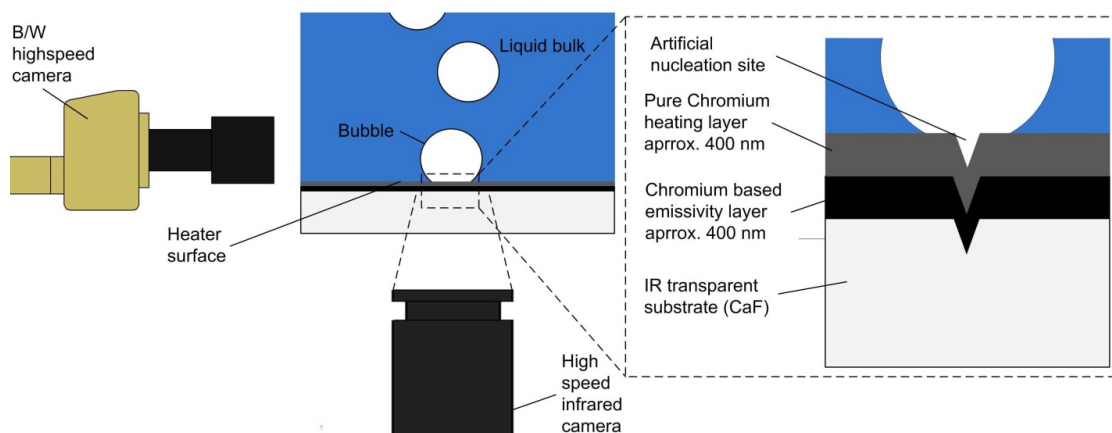


Fig. 4 Schematic of the thermal capacitive IR-transparent heater design

3. COMBINED GENERIC EXPERIMENTS AND SIMULATIONS AT THE AUTHORS' INSTITUTE

3.1 Experimental method and measurement technique

Single bubble experiments and simulations help to enhance our understanding of bubble growth and heat transfer. On realistic boiling surfaces bubble interaction will occur which might result in a change of the heat transfer characteristics. Consequently, single bubble experiments and simulations can only be a first step towards a more comprehensive understanding of boiling heat transfer. Recently, boiling experiments at twin cavities have been conducted at the author's institute to study the conditions under which bubble merging can occur and the implications for the local heat transfer. The experiments were accompanied by numerical simulations, to identify important parameters and bubble dynamics with high temporal and spatial resolution.

Results presented in section 3.3 were gained on two different heater assemblies. A thin foil heater, close to the design used by Kenning and Golobic, was used to investigate the effect of bubble coalescence. The foil surface was equipped with two artificial cavities at distances of 300 μm and 500 μm . To investigate the effect of the limited heat storage capability of the thin foil heaters and their low thermal capacity compared to technical heaters, a new thermal capacitive heater design has been developed, which allows the measurement of the heater surface temperature (Fischer et al., 2012a). In Fig. 4 a schematic sketch of the heater design and the measurement technique is shown. An IR transparent calcium fluoride (CaF_2) substrate is coated by Physical Vapor Deposition (PVD). The coating process itself is divided into two phases. The first phase provides a chromium based layer for better emissivity on the CaF_2 substrate, which is necessary to enhance the quality of the IR thermography measurement technique. As the thermal diffusivity of the CaF_2 substrate ($\alpha_{\text{CaF}} \approx 3.6\text{e-}6 \text{ m}^2/\text{s}$) is very close to that of stainless steel ($\alpha_{\text{Steel}} \approx 3.8\text{e-}6 \text{ m}^2/\text{s}$), the thermal transport in the heater substrate is very close to that in technical heaters. The second layer is a pure chromium layer, which is deposited on top of the chromium based layer, and which is used as electrical heating layer through Joule heating. The thickness of each layer is

about 400 nm, so the temperature measured by IR thermography on the backside of the chromium based emissivity layer is only $\sim 800 \text{ nm}$ away from the heater fluid interface. Because of their small thickness compared to the CaF_2 substrate thickness of 2 mm, the thermal resistance and the heat storage of the two-layer composition can be neglected. To control the position of bubble formation on the heater, the heaters were equipped with an artificial nucleation site. In both assemblies, the one with the thin foil heater and the one with the CaF_2 based heater, the general measurement method is the same (see Fig. 4). The temperature distribution close to the solid-fluid interface is measured using a high speed infrared IR camera. In case of the sputtered CaF_2 heater absorption and emission within the heater substrate can be neglected as the transmissivity of the heater substrate is 99.9 % for a thickness of 2 mm. Thus, the thermal radiation detected by the IR camera originates from the backside of the black layer. The electron count fields which are the output of the detector chip of the IR camera are mapped to the respective temperature through a pixel-wise in-situ calibration. To record the bubble shape, bubble movement and interaction, the IR camera is synchronized with a high-speed black and white camera that observes the fluid above the heater surface from the side.

For the thin foil heater, the local heat flux was calculated from the temperature fields using equation (1) with a finite differences approximation of the derivatives. While numerical evaluation has shown that the assumption of negligible temperature gradients across the heater thickness for the thin foil heater is justified, this assumption cannot hold true for the thermal capacitive IR transparent CaF_2 heater. To determine the heat flux in this case, a transient 3D energy balance for the heater substrate must be used:

$$\frac{\partial t}{\partial \tau} = \nabla(\alpha_s \nabla t) \quad (2)$$

Herein α_s is the thermal diffusivity of the IR transparent substrate. The entire substrate block is discretized into finite volumes and equation (2) is solved on this grid using the CFD-code OpenFOAM®. The preconditioned temperature fields are patched into the calculation as a transient boundary condition on top of the discretized

substrate. All other boundaries are considered to be adiabatic. As initial condition the substrate is assumed to be at a uniform temperature corresponding to the mean temperature of the first temperature field of a sequence. To ensure the stability of the calculation, the temperature fields are linearly interpolated in between the acquired frames, so more time steps can be performed. From this calculation one obtains the transient local heat flux distribution between the CaF₂ substrate and the chromium based emissivity layer, which has the same temporal and spatial resolution as the temperature field. By superposition of this heat flux field with the electrically generated heat flux within the pure chromium heating layer, the heat flux distribution at the heater-fluid interface is calculated. A discussion of the measurement accuracy and the subsequent uncertainty of further derived quantities using this method is presented by Fischer et al. (2012b). With both heaters PF-5060 was used as working fluid. The single bubble investigations on the thermal capacitive heater were also conducted in a low gravity environment during a parabolic flight. Due to the increased bubble growth period and bubble departure diameter under low gravity, the spatial and temporal resolution of a bubble growth and detachment process is increased compared to measurements under normal gravity.

3.2 Numerical Method

Currently, numerical simulations are based on the work of Kunkelmann and Stephan (2009). A standard 2-phase finite volume solver from the open source CFD Software OpenFOAM® was extended to allow the simulation of conjugate boiling heat transfer.

In the fluid domain the incompressible Navier-Stokes equations are solved with the PISO algorithm. In OpenFOAM®, the interface is tracked with the Volume-of-Fluid method (refer to Hirt and Nichols (1981)) and interface compression is applied to prevent the numerical diffusion of the interface. In the solid domain heat conduction is calculated and - depending on the problem definition - a volumetric heat source or temperature gradient at the bottom is applied. The solid and the fluid region are coupled by looping over the temperature equations and adjusting the boundary conditions in the solid and the fluid region. At the wall boundary, the temperature is fixed for the fluid region and the heat flux

is fixed for the solid region.

- The evaporative mass flux is calculated by the gradient based method described by Kunkelmann and Stephan (2010a). With this method, the temperature gradient close to the liquid-vapor interface is used to calculate the mass flux within each time step. The interface is assumed to be at saturation temperature at all times. An enthalpy sink in the temperature equation accordingly accounts for the heat of evaporation. The volume sources for the continuity equation are smeared by the method of Hardt and Wondra (2008) to prevent instabilities caused by large local volume sources. The following steps are performed to calculate the phase change: Calculation of the evaporative mass flux at the phase boundary
- Calculation of the energy source terms caused by evaporation for the energy equation
- Solving a diffusion equation for the evaporative mass flux
- Setting of mass sinks in the liquid region and mass sources in the vapor region
- Rescaling of mass sinks and sources, such that mass conservation is fulfilled

As mentioned, the thin film area in the vicinity of the contact line can play an important role in boiling processes and additional physics have to be considered. To capture the processes in this region, a subgrid scale model was implemented, which consists of a fourth order differential equation developed by Stephan and Busse (1992). As the calculation of a solution at each time step within the flow solver would be too time consuming, the calculations are performed with the software package Matlab® for several parameters. The results can be fitted by a series of root functions which are used in OpenFOAM®. The heat transferred within the contact line region is added directly to the calculation of the evaporation mass flux. For the conjugate problem, the heat transfer at the contact line can be added to the heat flux boundary of the solid region.

In OpenFOAM® the VoF method is used to track the movement of the phase boundary, which results in an interface that is smeared over several cells. In order to be able to accurately calculate the temperature gradient for the evaporation model, a contour based reconstruction of the interface was implemented by Kunkelmann and Stephan (2010b). The value of the VoF variable is interpolated from the cell centers to the points and assuming a linear gradient, the points where the VoF variable attains the value 0.5 can be calculated on the edges. With this

the interface normal and interface area can be determined for each cell. The reconstructed interface can furthermore be used to calculate the curvature of the interface, leading to a reduction in the velocities of the spurious

currents by one magnitude. Reducing the spurious currents is an important issue as they increase the heat transfer to the interface and therefore lead to an inaccurate quantitative calculation of the evaporation rate.

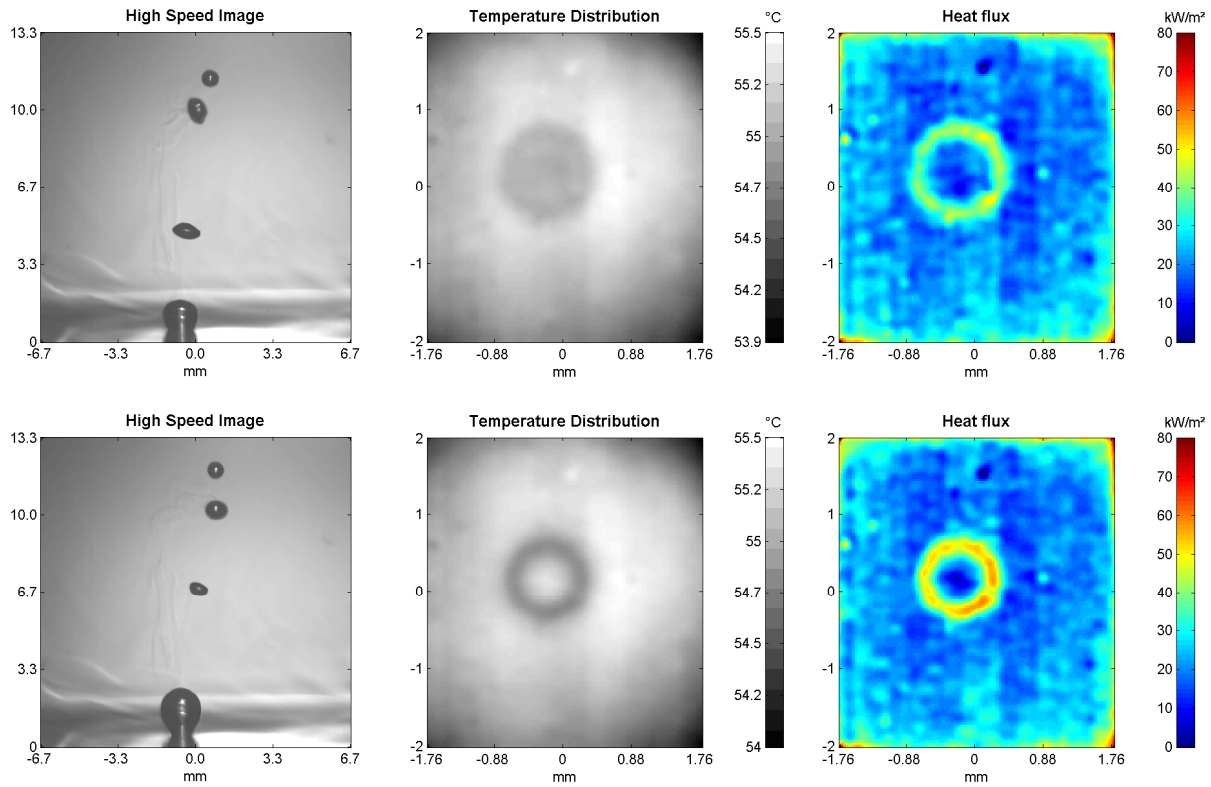


Fig. 5 High speed image, temperature distribution and heat flux below a vapor bubble growing on a CaF₂ heater during expansion of the bubble foot (upper row) and during contraction of the bubble foot (lower row) under lunar gravity (0.16 g_E)

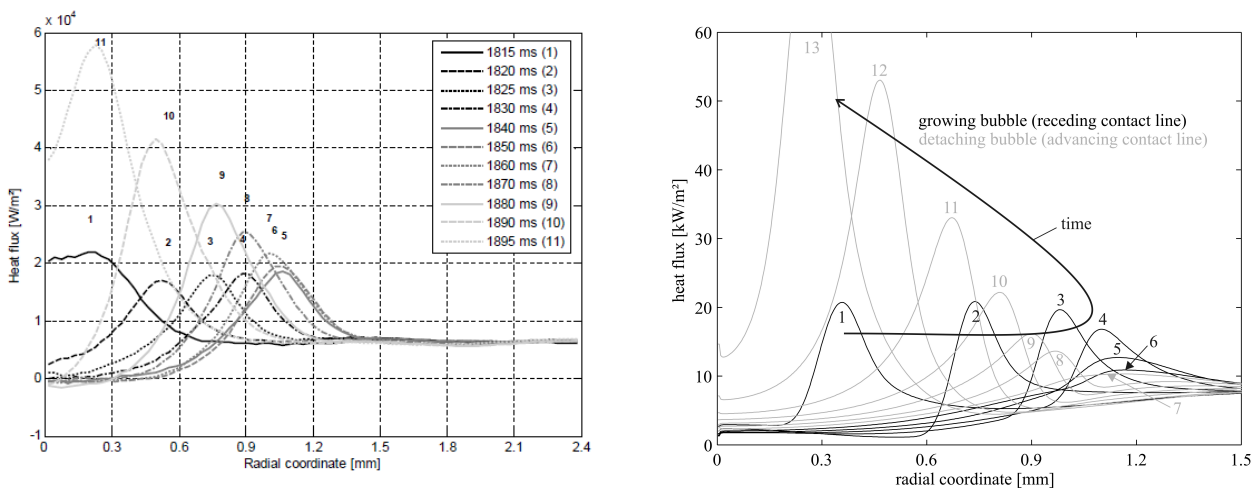


Fig. 6 Integrated heat flux at the 3-phase contact line of a single bubble, left: Experimental results (Schweizer, 2010), right: Numerical results (Kunkelmann, 2012)
The model allows full 3D simulations of boiling, evaporation and condensation processes. On hexahedral

cells OpenFOAM® offers dynamic mesh refinement options which can be employed to highly resolve the interface region without a massive increase in the overall number of cells. Furthermore, the model is fully parallelized to benefit from the capabilities of today's multi-core workstations and clusters.

The different parts of the model were validated extensively as described by Kunkelmann (2011). The performance of the full model was demonstrated by Kunkelmann and Stephan (2010a) by simulating nucleate boiling at a single nucleation site and comparing the results with experimental data of Wagner (2007).

Nucleation cannot be depicted with the numerical model. Therefore an initial bubble nucleus has to be set with the same frequency, as it is observed in the experiments. By simulating several cycles, the thermal boundary layer develops and consequently results are not depending on initial conditions. Bubble diameter and growth time were found to be within 20% of the experimental results. The temperature drop of the wall in the vicinity of the three phase contact line was 1.5 K for both, experiments and simulations.

3.3 Results

In Fig. 5 a typical result from measurements carried out on the IR transparent heater element as described in section 3.1 is shown for an expanding bubble foot (receding contact line, Fig. 5, upper row) and a contracting bubble foot (advancing contact line, Fig. 5, lower row). As it has been observed for foil heaters, the distinct heat flux peak in close proximity of the 3-phase contact line is also visible for this heater configuration. When comparing these results to those obtained by Schweizer and Stephan (2009), one can notice that the temperature drop in the heater substrate caused by the bubble is one order of magnitude lower. This difference is caused by the much higher thermal capacity of the CaF₂ heater compared to the thin foil heater used by Schweizer and Stephan (2009). However, the location of the temperature drop detected by the IR camera is much more bounded by steep temperature gradients on the CaF₂ heater. This is caused by the differences in the measurement plane. While the location of the temperature measurement on the thin foil heater is 10 μm or 20 μm away

from the heater-fluid interface (depending on the thickness of the foil) the measurement plane of the CaF₂ heater is only ~800 nm away from the interface. Therefore the temperature signal on the thin foil heater is blurred through lateral thermal conduction across the foil thickness, while there is only very small blurring across the two sputtered layers of the CaF₂ heater. The initial stages of bubble growth are accompanied by high contact line velocities, removing energy from the substrate faster than it can be re-supplied through thermal conduction.

This results in an apparently global temperature drop below the growing bubble as seen in the upper row of Fig. 5. As the bubble foot reaches its maximum radius, the contact line velocity is slowed down and the temperature drop below the bubble is compensated by thermal conduction within the solid. At the 3-phase contact line however, energy is still constantly removed by contact line evaporation, resulting in a very narrow temperature drop close to the contact line (see Fig. 5, lower row). For the low receding contact line velocity during the contraction of the bubble foot, this temperature minimum close to the contact line stays localized until bubble departure. The local heat flux peak at the 3-phase contact line is even higher in this case than in case of the expanding bubble foot. This result is in agreement with previous experimental investigation carried out on thin foil heaters by Schweizer (2010), even though distinctive differences in the thermal response of the solid were found. The results obtained by Schweizer (2010) are in very good agreement to numerical calculations by Kunkelmann (2011). In Fig. 6 a comparison of experimental and numerical results for the integrated heat flux at the contact line of single bubbles is shown. Numerical simulations of moving 3-phase contact lines by Kunkelmann et al. (2012) indicate that the reason for higher heat flux during the advancing contact line situation is that cold liquid is sucked to the heater surface through the motion of the liquid vapor interface; see Fig. 7. As can be seen in the Fig. the highest temperature gradient occur either close to the wall-liquid interface (advancing contact line during detaching bubble phase) or close to the liquid-vapor interface (receding contact line during growing bubble phase). Furthermore, the dry wall below the bubble heats up and thus the temperature differences between wall

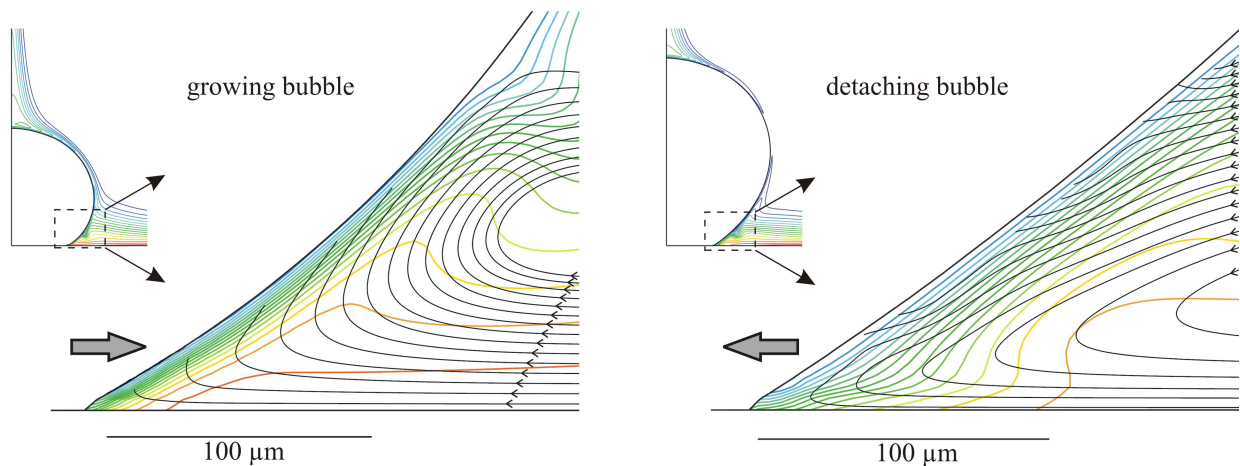


Fig. 7 Temperature field (colored curves, distance: 1 K) and streamlines of relative velocity (black curves) in close vicinity of the 3-phase contact line during bubble growth (4 ms after nucleation) and detachment (10 ms after nucleation) (Kunkelmann, 2011)

and saturated liquid are higher for the advancing contact line than for the receding one. A real heater element usually has a rather high thermal capacity. This experiment proves that in such a case the transient heat transfer within the solid material cannot be neglected, as it has a strong effect onto the local temperature and heat flux distribution during the early stages of a bubble cycle.

From the experiments with two artificial cavities it was possible to show that for a given distance of the cavities, an optimal pressure exists to maximize the probability of bubble merging to occur. In Fig. 8 the optimal pressure for two different cavity spacings is shown. If pressure is much lower or much higher than the optimal pressure bubble coalescence rarely occurs. At low pressures the nucleation site that is activated first creates a fast growing bubble that covers immediately the second nucleation site. Thus, only a single large bubble is observed. At high pressures bubble departure diameters are much smaller, consequently, two bubbles are generated and growing next to each other without coalescence. Therefore the optimal pressure for coalescence rises with decreasing cavity distance.

During experiments with the thin foil heater at pressures below 600 mbar a residual liquid droplet was observed within the large bubble that was generated during the merging process of the two small bubbles. The formation of this droplet could be reproduced within nu-

merical simulations.

A comparison of the heat flux obtained from numerical simulations and from experiments is shown in Fig. 9. From the numerical results it could be withdrawn that after the bubble merger a capillary wave at the liquid-vapor interface propagates from the merging plane along the bubble surface. The fast movement of the liquid-vapor interface and the 3-phase contact line following the merging process leads to a local enhancement of the heat flux. This local heat flux enhancement can be observed in Fig. 9 at the right and the left hand side of the bubble at 4 ms and 6 ms after the merging event.

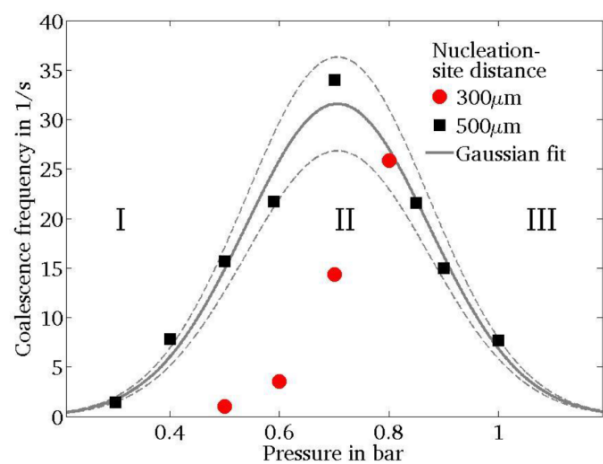


Fig. 8 Frequency of horizontal bubble coalescence

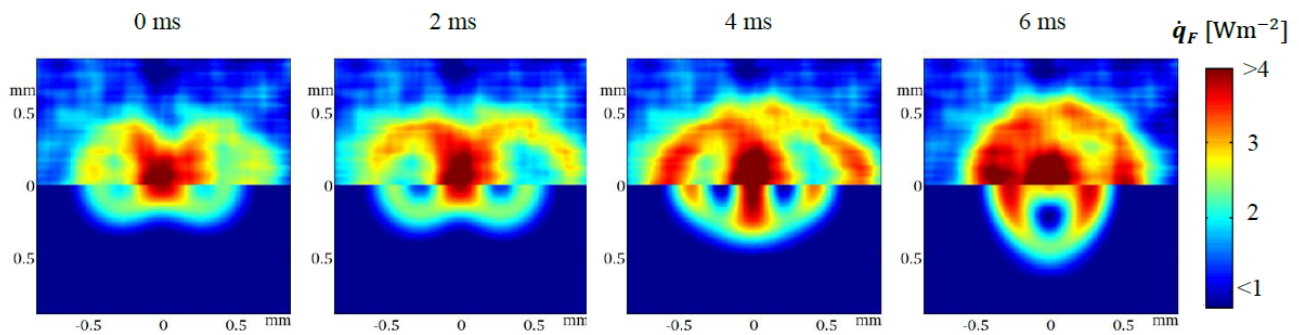


Fig. 9 Comparison of experimental (top) and numerical (bottom) heat flux profile during coalescence

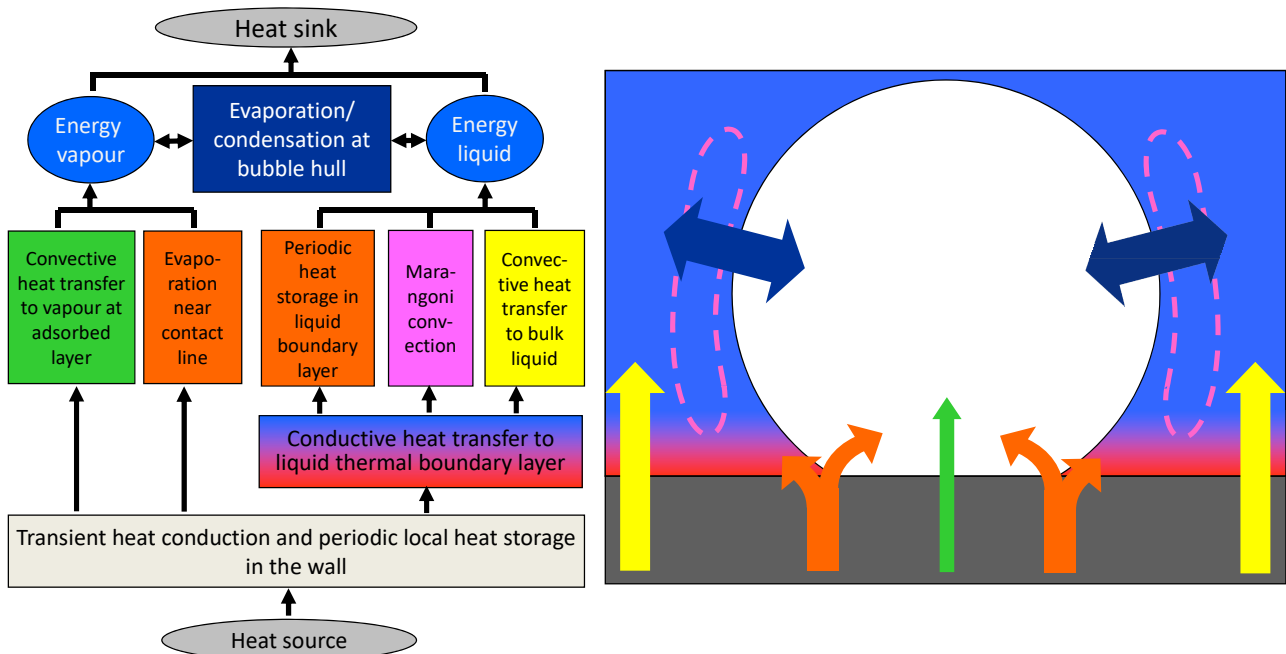


Fig. 10 Heat paths from heater (heat source) to bulk fluid (heat sink) during a single bubble cycle of the nucleate boiling process

4. CONCLUSIONS ON LOCAL TRANSPORT PHENOMENA: LEARNING OUTCOME

Heat transfer and evaporation at a single bubble subsystem seems to represent nucleate boiling phenomena quite well up to about 40 to 50% of the critical heat flux. Above this heat flux bubble interactions and flow dynamics become more important. On the basis of numerous previous studies and the recently performed combined generic single bubble experiments and numerical

simulations the following conclusions on local transport phenomena can be drawn. The related heat paths from heat source (heater) to heat sink (bulk fluid) are schematically shown in Fig. 10.

- Local transient effects in heat conduction in the wall underneath the bubble are quite pronounced. Therefore, numerical models assuming constant and homogeneous wall temperature do not depict an important effect. During the bubble growth and departure phase the wall is locally cooled down. A minimum temperature is observed underneath the moving contact line with large local temperature gradients. During the bubble rise phase and waiting

period the wall next to the nucleation site is reheated again.

- The near contact line region evaporation accounts for up to approx. 30% of the overall evaporation rate during a complete bubble cycle. During the growth phase with increasing bubble base radius (receding contact line) the local heat flux maximum is less pronounced than during the bubble departure phase with decreasing base radius (advancing contact line).
- Convective heat transfer from the wall to the liquid boundary layer next to the bubble accounts for at least approx. 70% of the overall heat rejection from the wall.
- Direct convective heat transfer from the wall to the vapor at the dry patch (adsorbed thin film) underneath the bubble contributes only very little to the overall heat transfer.
- The evaporation rate decreases dramatically during the bubble rise phase. Recondensation might occur depending on the subcooling of the bulk liquid.
- The liquid boundary layer is cooled down during the bubble growth and departure phase due to strong evaporation. During the departure and the initial rise phase cold liquid flows from the bulk area into the wake of the bubble. Later the liquid boundary layer next to the nucleation site locally heats up again until nucleation occurs again.
- Marangoni convection due to temperature gradient can be neglected for pure fluids. Opposed to that, Marangoni convection due to composition gradient in mixtures might be relevant.

Further studies, both, generic experiments as well as numerical simulations, are needed. Attention should be directed towards the phenomena during bubble mergers to expand the knowledge of heat transfer phenomena described in this paper towards higher heat flux regimes. Understanding heterogeneous nucleation is still a totally open issue, and predictions of active nucleation site densities are therefore impossible. Much work is needed here.

ACKNOWLEDGMENT

The authors acknowledge the financial support of their boiling research projects by the German Science Foundation DFG and the European Space Agency ESA during the last years. The first author, Peter Stephan, also thanks the Heat Transfer Society of Japan and its international evaluation board for awarding the Nukiyama Memorial Award to him. This paper was presented within bestowal

of the award.

REFERENCES

- Aktinol, E. and Dhir, V.K., Numerical Simulation of Nucleate Boiling Phenomenon Coupled with Thermal Response of the Solid, *Microgravity Sci. Tech.*, Vol. 24, pp. 225-265, 2012.
- Arlabosse, P., Tadrist, L., Tadrist, H. and Pantaloni, J., Experimental Analysis of the Heat Transfer Induced by Thermocapillary Convection Around a Bubble, *J. Heat Transf.*, Vol. 122, pp. 66-73, 2000.
- Auracher, H. and Buchholz, M., Experiments on the fundamental mechanisms of boiling heat transfer, *J. Braz. Soc. Mech. Sci.*, Vol. 27, 2005.
- Bai, Q. and Dhir, V.K., Numerical Simulation of Bubble Dynamics in the Presence of Boron in the Liquid, *Proceedings of 2001 ASME International Mechanical Engineering Congress and Exposition*, New York, 2001.
- Bai, Q. and Fujita, Y., Numerical Simulation of Bubble Growth in Nucleate Boiling - Effect of System Parameter, *Proc. Int. Boiling Conference, Boiling 2000: Phenomena & Emerging Applications*, pp. 149-155, Anchorage, Alaska, USA, April 30-May 5, 2000.
- Barthès, M., Reynard, C., Santini, R. and Tadrist, L., Experimental Study of a Single Vapour Bubble Growth: Heat and Mass Transfer Analysis – Influence of Non-Condensable Presence on the Onset of Marangoni Convection, *Proc. of the 13th International Heat Transfer Conference IHTC13*, Sydney, Australia, August 13-18, 2006.
- Brackbill, J.U., Kothe, D.B. and Zemach, C., A continuum method for modeling surface tension, *J. Comput. Phys.*, Vol. 100, pp. 335-354, 1992.
- Delgoshaei, P. and Kim, J., Microscale Heat Transfer Measurements during subcooled Pool Boiling of pentane: Effect of Bubble Dynamics, *Proc. of the 14th International Heat Transfer Conference IHTC14*, Washington DC, USA, August 8-13, 2010.
- Dhir, V. K., Numerical Simulations of Pool-Boiling Heat Transfer, *AIChE Journal*, Vol. 47, pp. 813-834, 2001.
- Dhir, V. K., Warriar, G. R., Aktinol, E., Chao, D., Eggers, J., Sheredy, W. and Booth, W., Nucleate Pool Boiling Experiments (NPBX) on the International Space Station, *Microgravity Sci. Tech.*, Vol. 24, pp. 1-19, 2012.

Di Marco, P. and Grassi, W., Motivation and results of a long-term research on pool boiling heat transfer in low gravity, *Intern. J. Therm. Sci.*, Vol. 41, pp. 567–585, 2002.

Di Marco, P., Grassi, W., Memoli, G., Takamasa, T., Tomiyama, A. and Hosokawa, S., Influence of electric field on single gas-bubble growth and detachment in microgravity, *Intern. J. Multiphas. Flow*, Vol. 29, pp. 559–578, 2003.

Di Marco, P., Giannini, N., Saccone, G., Experimental Determination the Forces acting on a growing Gas Bubble in Quasi-static Conditions, *Proc. of the ECI 8th International Conference on Boiling and Condensation Heat Transfer*, Lausanne, Switzerland, June 3-7, 2012a.

Di Marco, P., The Use of Electric Force as a Replacement of Buoyancy in Two-phase Flow, *Microgravity Sci. Tech.*, Vol. 24, pp. 215–228, 2012b.

Duan, X., Phillips, B., McKrell, T and Buongiorno, J., Synchronized high speed video, infrared thermometry and PIV data for validation of interface-tracking simulations of nucleate boiling phenomena, *Proc. of the ECI 8th International Conference on Boiling and Condensation Heat Transfer*, Lausanne, Switzerland, June 3-7, 2012.

Esmaceli, A. and Tryggvason, G., A front tracking method for computations of boiling in complex geometries, *Intern. J. Multiphas. Flow*, Vol. 30, pp. 1037-1050, 2004.

Fischer, S., Herbert, S., Sielaff, A., Slomski, E. M., Stephan, P. and Oechsner, M., Experimental Investigation of Nucleate Boiling on a Thermal Capacitive Heater Under Variable Gravity Conditions, *Microgravity Sci. Tech.*, Vol. 24, pp. 139–146, 2012a.

Fischer, S. Herbert, S., Slomski, E. M., Stephan, P. and Oechsner, M., Local Heat Flux Investigation during Pool Boiling Single Bubble Cycles under Reduced Gravity, *Proc. of the ECI 8th International Conference on Boiling and Condensation Heat Transfer*, Lausanne, Switzerland, June 3-7, 2012b.

Fuchs, T., Kern, J. and Stephan, P., A Transient Nucleate Boiling Model Including Microscale Effects and Wall Heat Transfer, *J. Heat Transf.*, Vol. 128, pp. 1257-1265, 2006.

Geradi, C. Buongiorno, J, Hhu, L. and McKrell, T.,

Measurement of nucleation site density, bubble departure diameter and frequency in pool boiling of water using high-speed infrared and optical cameras, *Proc. of 7th ECI International Conference on Boiling and Condensation Heat Transfer*, Brazil, May 3-7, 2009.

Geradi, C., Buongiorno, J., Hu, L. and McKrell, T., Study of bubble growth in water pool boiling through synchronized, infrared thermometry and high-speed video, *Intern. J. Heat Mass Tran.*, Vol.53, pp. 4185-4192, 2010.

Golobic, I. and Gjerkes, H., Interaction between laser-activated nucleation sites in pool boiling, *Intern. J. Heat Mass Tran.*, Vol. 44, pp. 143-153, 2001.

Golobic, I., Petkovsek, J., Baselj, M., Papez, A. and Kenning, D. B. R., Experimental determination of transient wall temperature distribution close to growing vapor bubbles, *Heat Mass Transfer*, Vol. 45, pp. 857-866, 2009.

Golobic, I., Petkovsek, J. and Kenning, D. B. R., Bubble growth and horizontal coalescence in saturated pool boiling on a titanium foil, investigated by high-speed IR thermography, *Int. J. Heat Mass Transf.*, Vol. 55, pp. 1385-1402, 2012.

Hardt, S. and Wondra, F., Evaporation model for interfacial flows based on a continuum-field representation of the source terms, *J. Comput. Phys.*, Vol. 227, pp. 5871–5895, 2008.

Harlow, F.H. and Welch, J.E., Numerical calculation of time-dependent viscous incompressible flow of fluid with free surface, *Phys. Fluids*, Vol. 8, pp. 2182-2189, 1965.

Heng, Y., Mhamdi, A., Groß, S., Reusken, A., Buchholz, M., Auracher, H. and Marquardt, W., Reconstruction of local heat fluxes in pool boiling experiments along the entire boiling curve from high resolution transient temperature measurement, *Intern. J. Heat Mass Tran.*, Vol. 51, pp. 5072-5087, 2008.

Heng, Y., Mhamdi, A. and Marquardt, W., Efficient reconstruction of local heat fluxes in pool boiling experiments by goal-oriented adaptive mesh refinement, *Heat Mass Transfer*, Vol. 46, pp. 1121-1135, 2010.

Heng, Y., Karalashvili, M., Mhamdi, A. and Marquardt, W., A multi-level adaptive solution strategy for 3D inverse problems in pool boiling, *Int. J. Numer. Method H.*, Vol. 21, pp. 469-493, 2011.

Hirt, C.W. and Nichols, B.D., Volume of fluid (VOF) method for the dynamics of free boundaries, *J. Comput. Phys.*, Vol. 39, pp. 201-225, 1981.

Hutter, C., Kenning, D. B. R., Sefiane, K., Karayiannis, T. G., Lin, H., Cummins, G. and Walton, A. J., Experimental pool boiling investigations of FC-72 on silicon with artificial cavities and integrated temperature microsensors, *Exp. Therm. Fluid Sci.*, Vol. 34, pp. 422-433, 2010.

Hutter, C., Sefiane, K., Karayiannis, T. G., Walton, A., Nelson, R. A. and Kenning, D. B. R., Nucleation site interaction between artificial cavities during nucleate pool boiling on silicon with integrated micro-heater and temperature micro-sensors, *Intern. J. Heat Mass Tran.*, Vol. 55, pp. 2769-2778, 2012.

Kenning, D. B. R. and Yan, Y., Pool boiling heat transfer on a thin plate : features revealed by liquid crystal thermography, *Intern. J. Heat Mass Tran.*, Vol. 39, pp. 3117-3137, 1996.

Kenning, D. B. R., Kono, T. and Wienecke, M., Investigation of boiling heat transfer by liquid crystal thermography, *Exp. Therm. Fluid Sci.*, Vol. 25, pp. 219-229, 2001.

Kenning, D. B. R. and Bustnes, O.-E., Liquid crystal studies of sliding vapour bubbles, *Heat Mass Transfer*, Vol. 45, pp. 867-888, 2009.

Kern, J. and Stephan, P., Theoretical Model for Nucleate Boiling Heat Transfer of Binary Mixtures, *J. Heat Transf.*, Vol. 125, pp. 1106-1115, 2003.

Kim, J., John F. Benton, J. F. and Wisniewski, D., Pool boiling heat transfer on small heaters: effect of gravity and subcooling, *Intern. J. Heat Mass Tran.*, Vol. 45, pp. 3919-3932, 2002.

Kim, H. and Buongiorno, J., Development of an infrared-based visualization technique to study phase dynamics on boiling surfaces, *Proceedings of the 4th International Conference on Heat Transfer and Fluid Flow in Microscale*, Japan, 2011a.

Kim, H. and Buongiorno, J., Detachment of liquid-vapour-solid triple contact line in two-phase heat transfer phenomena using high-speed infrared thermometry, *Intern. J. Multiphas. Flow*, Vol. 37, pp. 166-172, 2011b.

Kunkelmann, C. and Stephan, P., CFD Simulation of Boiling Flows Using the Volume-of-Fluid Method within

OpenFOAM, Proc. of 7th ECI International Conference on Boiling and Condensation Heat Transfer, Brazil, May 3-7, 2009.

Kunkelmann, C. and Stephan, P., Numerical simulation of the transient heat transfer during nucleate boiling of refrigerant HFE-7100, *Int. J. Refrig.*, Vol. 33, pp. 1221-1228, 2010a.

Kunkelmann, C. and Stephan, P., Modification and Extension of a Standard Volume-of-Fluid Solver for Simulating Boiling Heat Transfer, Proc. of the 5th European Conference on Computational Fluid Dynamics, Lisbon, Portugal, June 14 – 17, 2010b.

Kunkelmann, C., Numerical Modeling and Investigation of Boiling phenomena, PhD thesis, URL: <http://tuprints.ulb.tu-darmstadt.de/2731/>, Technische Universität Darmstadt, 2011.

Kunkelmann, C., Ibrahim, K., Schweizer, N., Herbert, S., Stephan, P. and Gambaryan-Roisman, T., The effect of three-phase contact line speed on local evaporative heat transfer: Experimental and numerical investigations, *Int. J. Heat Mass Transf.*, Vol. 55, pp. 1896-1904, 2012.

Lay, J.H. and Dhir, V.K., Shape of a Vapor Stem During Nucleate Boiling of Saturated Liquids, *J. Heat Transf.*, Vol. 117, pp. 394-401, 1995.

Nukiyama, S., The Maximum and Minimum Values of the Heat Q Transmitted from Metal to Boiling Water under Atmospheric Pressure, *J. Japan Soc. Mech. Eng.*, Vol. 37, no. 206, pp. 367-374, 1934. (english translation: *Int. J. Heat Mass Transf.*, Vol. 9, pp. 1419-1433, 1966, and Vol. 27, pp. 959-970, 1984).

Manglik, R.M., On the Advancements in Boiling, Two-Phase Flow Heat Transfer, and Interfacial Phenomena, *J. Heat Transf.*, Special Issue on Boiling Heat Transfer, Vol. 128, pp. 1237-1242, 2006.

Mukherjee, A. and Dhir, V.K., Study of Lateral Merger of Vapor Bubbles During Nucleate Pool Boiling, *J. Heat Transf.*, Vol. 126, pp. 1023-1039, 2004.

Mukherjee, A. and Kandlikar, S.G., Numerical study of single bubbles with dynamic contact angle during nucleate pool boiling, *Intern. J. Heat Mass Tran.*, Vol. 50, pp. 127-138, 2007.

Osher, S. and Sethian, J.A., Fronts propagating with curvature dependent speed: Algorithms based on Hamilton-Jacobi formulations, *J. Comput. Phys.*, Vol. 79, pp. 12-49, 1988.

Potash, M. and Wayner, P., Evaporation from a two-dimensional extended meniscus, *Intern. J. Heat Mass Tran.*, Vol. 15, pp. 1851-1863, 1972.

Qiu, D. M., Dhir, V. K., Chao, D., Hasan, M. M., Neumann, E., Yee, G. and Birchenough, A., Single-Bubble Dynamics During Pool Boiling Under Low Gravity Conditions, *J. Thermophys. Heat Tr.*, Vol. 16, pp. 336-345, 2002.

Raj, R. and Kim, J., Heater Size and Gravity Based Pool Boiling Regime Map: Transition Criteria Between Buoyancy and Surface Tension Dominated Boiling, *J. Heat Transf.*, Vol. 132, pp. 091503-1 - 091503-10, 2010a.

Raj, R., Kim, J. and McQuillen, J., Gravity Scaling Parameter for Pool Boiling Heat Transfer, *J. Heat Transf.*, Vol. 132, pp. 091502-1-091502-9, 2010b.

Reynard, C., Santini, R. and Tadrist, L., Experimental study of the gravity influence on the periodic thermocapillary convection around a bubble, *Exp. Fluids*, Vol. 31, pp. 440-446, 2001.

Reynard, C., Barthès, M., Santini, R. and Tadrist, L., Experimental study of the onset of the 3D oscillatory thermocapillary convection around a single air or vapor bubble. Influence on heat transfer, *Exp. Therm. Fluid Sci.*, Vol.29, pp. 783-793, 2005.

Schweizer, N. and Stephan, P.: Experimental Study of Bubble Behavior and local Heat flux in Pool boiling under variable gravitational Conditions, *Multiphase Sci. Tech.*, Vol. 21, pp. 329-350, 2009.

Schweizer, N., Multiscale investigation of nucleate boiling phenomena in microgravity, PhD thesis, URL <http://tuprints.ulb.tu-darmstadt.de/2377/>, Technische Universität Darmstadt, 2010.

Siedel, S., Cioulachtjian, J. and Bonjour, J., Experimental analysis of bubble growth, departure and interactions during pool boiling on artificial nucleation sites, *Exp. Therm. Fluid Sci.*, Vol. 32, pp. 1504-1511, 2008.

Sodtke, C., Schweizer, N., Wagner, E. and Stephan, P., Experimental Study of Nucleate Boiling Heat Transfer under low Gravity Conditions using TLCs for High Resolution Measurements, *Proc. of the ECI 6th International Conference on Boiling Heat Transfer*, Spoleto, Italy, May 7-12, 2006a.

Sodtke, C., Kern, J., Schweizer, N., Stephan, P., High resolution measurements of wall temperature distribution underneath a single vapour bubble under low gravity

conditions, *Intern. J. Heat Mass Tran.*, Vol. 49, pp. 1100-1106, 2006b.

Son, G. and Dhir, V.K. and Ramanujapu, N., Dynamics and Heat Transfer Associated With a Single Bubble During Nucleate Boiling on a Horizontal Surface, *J. Heat Transf.*, Vol. 121, pp. 623-631, 1999.

Son, G., Ramanujapu, N. and Dhir, V.K., Numerical Simulation of Bubble Merger Process on a Single Nucleation Site During Pool Nucleate Boiling, *J. Heat Transf.*, Vol. 124, pp. 51-62, 2002.

Stephan, P. and Busse, C., Analysis of the heat transfer coefficient of grooved heat pipe evaporator walls, *Intern. J. Heat Mass Tran.*, Vol. 35, pp. 383-391, 1992.

Stephan, P. and Hammer, J., A new model for nucleate boiling heat transfer, *Heat and Mass Transfer*, Vol. 30, pp. 119-125, 1994.

Theofanous, T. G., Tu, J. P., Dinh, A. T. and Dinh, T.N., the boiling crisis phenomenon Part II: dryout dynamics and burnout, *Exp. Therm. Fluid Sci.*, Vol. 26, pp. 793-810, 2002.

Wagner, E., Stephan, P., Koeppen, O. and Auracher, H., High resolution temperature measurements at moving vapor/liquid and vapor/liquid/solid interfaces during bubble growth in nucleate boiling, *Proceeding of the 4th International Berlin Workshop on Transport Phenomena with Moving Boundaries*, VDI Verlag, pp. 260-277, 2007.

Wagner, E. and P. Stephan, P., Experimental Study of local Temperature Distribution and Heat Transfer Mechanisms during Nucleate Boiling of binary Mixtures, *Proc of the 5th European Thermal-Sciences Conference EU-ROTHERM 2008*, Eindhoven, the Netherlands, 18-22 May, 2008.

Welch, S.W.J, Direct simulation of vapor bubble growth, *Intern. J. Heat Mass Tran.* Vol. 41, pp. 1665-1666, 1998.

Wu, J., Dhir, V.K., and Qian, J., Numerical Simulation of Subcooled Nucleate Boiling by Coupling Level-Set Method with Moving-Mesh Method, *Num. Heat Tr. B-Fund.*, Vol. 51, pp. 535-563, 2007.

Wu, J. and Dhir, V.K., Numerical Simulations of the Dynamics and Heat Transfer Associated With a Single Bubble in Subcooled Pool Boiling, *J. Heat Transf.*, Vol. 132, 111501-15, 2010.

Yoon, H.Y., Koshizuka, S. and Oka, Y., Direct calcu-

lation of bubble growth, departure, and rise in nucleate pool boiling, *Int. J. Multiphase Flow*, Vol. 27, pp. 277-298, 2007.
